Supporting Information for

General Synthesis of Magnetic Binary Transition Metal Telluride Nanocrystals

Jingxia Wang[a], Bin Wang[a], Yifen Wang[a], Ruixia Yang[a], Lanfang Wang[a], Fang Wang[a], Xiaohong, Xu[a], and Yang Liu[b,*]

[a]Research Institute of Materials Science of Shanxi Normal University & Key Laboratory of Magnetic Molecules and Magnetic Information Materials of Ministry of Education, Taiyuan 030031, China.

[b]Department of Materials Science, Fudan University, Shanghai 200433, China.

[*]Correspondence should be addressed to Yang Liu (liuyang_fd@fudan.edu.cn)

Table S1. Summary of experimental parameters used for the synthesis of metal telluride NCs.

	metal precursor	M:Te molar ratio	Reaction time (min)	Reaction temperature (°C)	Product NCs
Ni-Te	$Ni(acac)_2$	1:2	5	250	$NiTe_2$
		1:2	5	300	$NiTe_2$
		1:2	60	330	$NiTe_2$
		1:1.5	5	250	$Ni_{0.75}Te$
		1:1.5	5	300	$Ni_{0.64}Te$
		1:1.5	60	330	$Ni_{0.53}Te$
		1:1	5	250	NiTe
		1:1	5	300	NiTe
		1:1	60	330	$Ni_{0.88}Te$
	$Ni(OAc)_2$	1:2	60	330	$NiTe_2$
		1:1.5	60	300	$Ni_{0.64}Te$
	$NiCl_2$	1:2	60	330	$NiTe_2$
		1:1.5	60	300	$Ni_{0.64}Te$
Co-Te	$Co(acac)_2$	1:2	60	300	$CoTe_2$
		1:2	60	330	$CoTe_2$
		1:1.5	5	250	$CoTe_2$
		1:1.5	5	300	$CoTe_2$
		1:1.5	60	330	$Co_{0.64}Te$
		1:1	5	250	$CoTe_2$
		1:1	5	300	$CoTe_2$
		1:1	60	330	CoTe
	$Co(OAc)_2$	1:2	60	330	$CoTe_2$
		1:1.5	60	330	$Co_{0.67}Te$
		1:1	60	330	$Co_{0.83}Te$
	$CoCl_2$	1:2	60	330	$CoTe_2$

Fe-Te	$Fe(acac)_3$	1:2	60	300	$FeTe_2$
	$Fe(OAc)_2$	1:2	60	330	$FeTe_2$
	$FeCl_3$	1:2	60	300	$FeTe_2$
	$FeCl_2$	1:2	60	300	$FeTe_2$
Mn-Te	$Mn(acac)_2$	1:2	120	330	$MnTe_2$
		1:1.5	120	330	$MnTe_2$
		1:1.5	60	330	$MnO+MnTe_2$
		1:1.5	45	330	$MnO+MnTe_2$
		1:1.5	30	330	MnO
		1:1	120	330	$MnO+MnTe_2$
	$Mn(acac)_3$	1:2	120	330	$MnO+MnTe_2$
		1:2	120	300	MnO
	$Mn(OAc)_2$	1:2	120	330	MnO
	$MnCl_2$	1:2	30	300	No product
Cr-Te	$Cr(CO)_6$	1:1.8	120	350	Cr_2Te_3
	$Cr(acac)_3$	1:1.8	120	350	No product
	$CrCl_3$	1:1.8	120	350	No product
	$CrCl_2$	1:1.8	120	350	No product

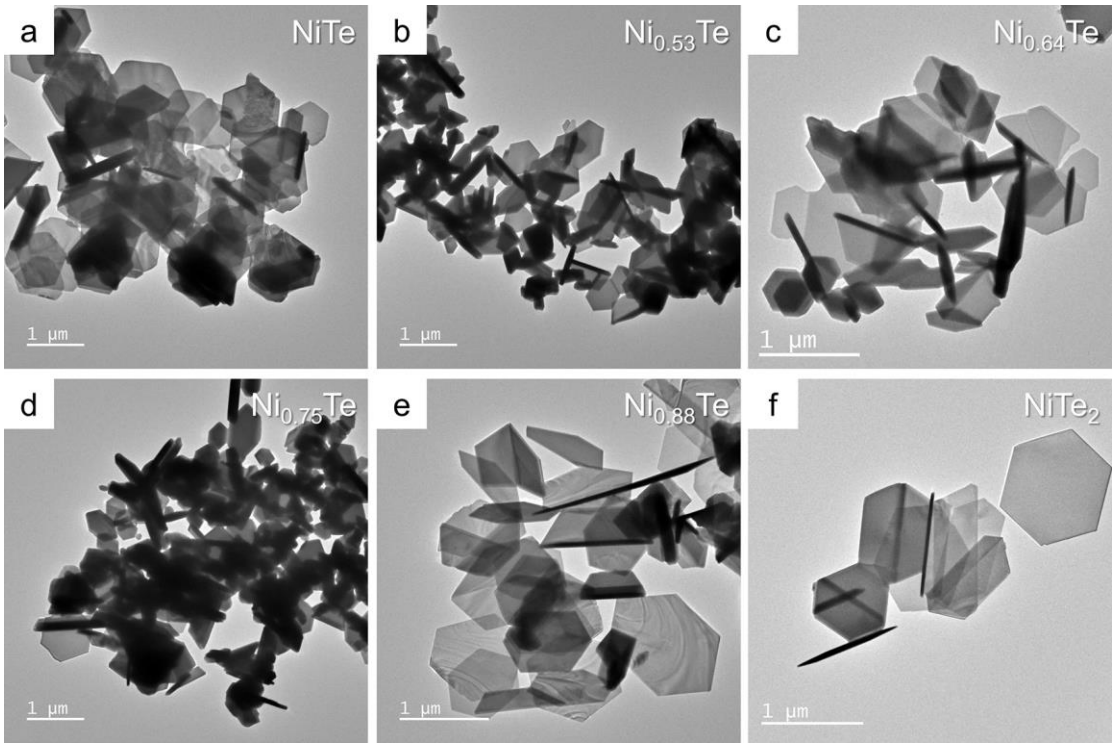

Fig. S1. TEM images different $NiTe_{2-x}$ nanosheets synthesized using $Ni(acac)_2$ precursor.

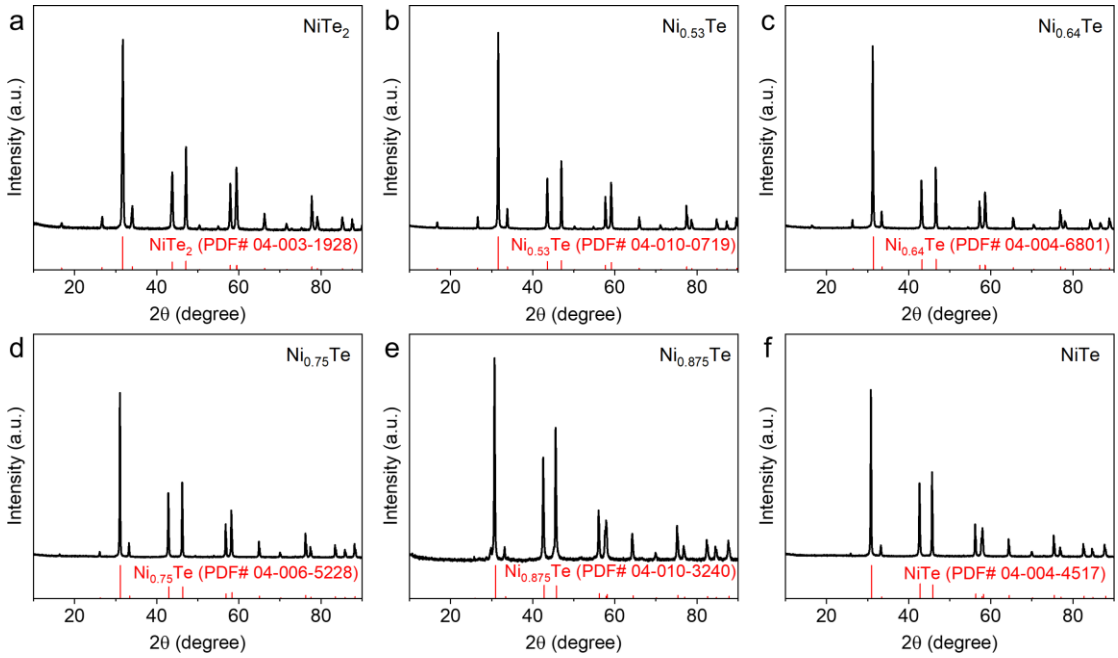

Fig. S2. XRD patterns of $NiTe_{2-x}$ nanosheets: (a) $NiTe_2$, (b) $Ni_{0.53}Te$, (c) $Ni_{0.64}Te$, (d) $Ni_{0.75}Te$, (e) $Ni_{0.88}Te$, (f) NiTe.

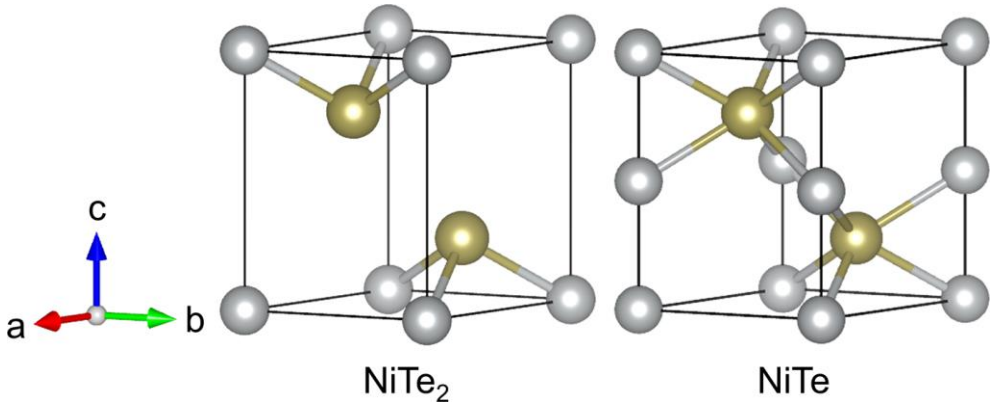

Figure S3. Structural models of $NiTe_2$ and NiTe.

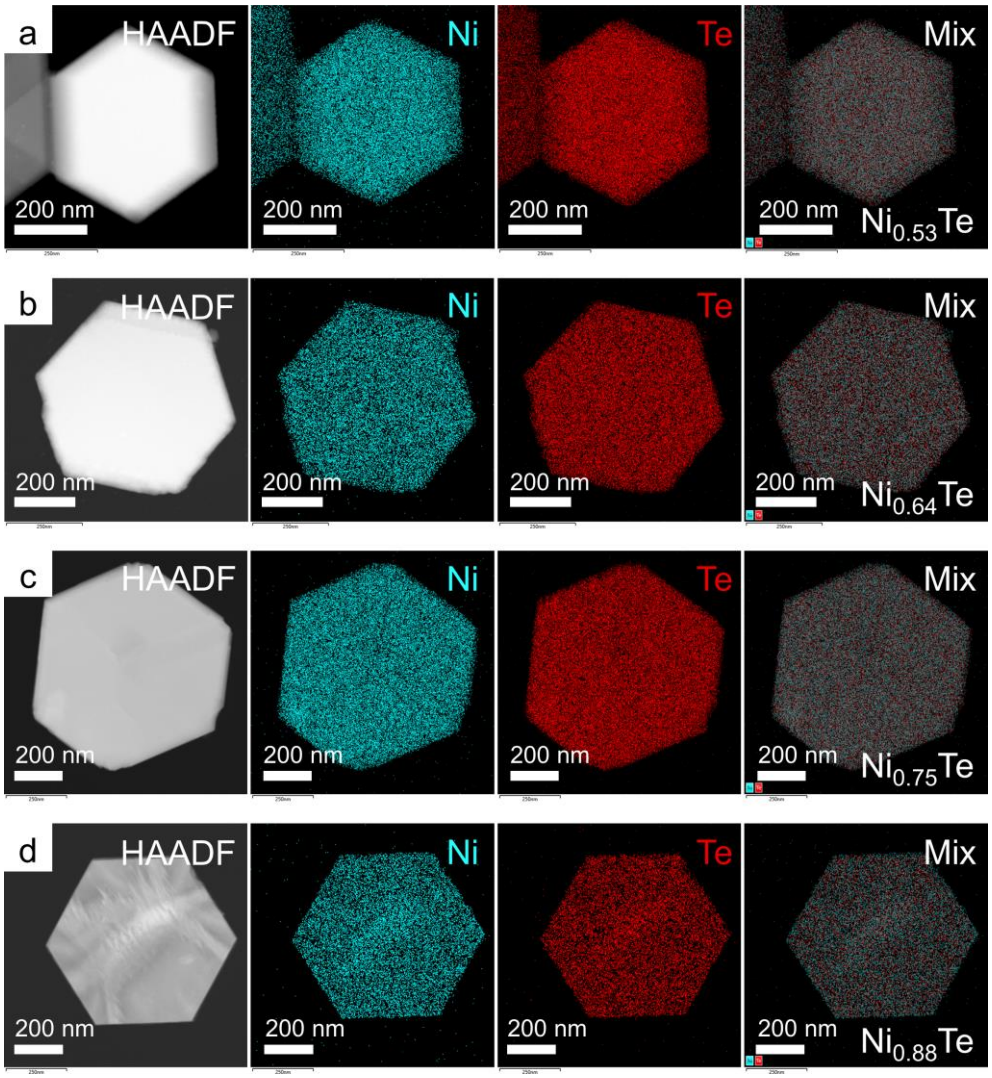

Fig. S4. HAADF and elemental maps of Ni and Te for (a) $Ni_{0.53}Te$, (b) $Ni_{0.64}Te$, (c) $Ni_{0.75}Te$, (d) $Ni_{0.88}Te$.

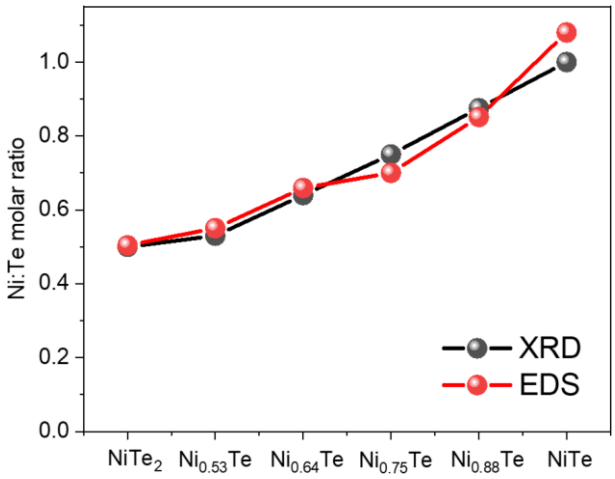

Fig. S5. Comparison of the Ni:Te molar ratio in various $NiTe_{2-x}$ based on quantitative EDS results and XRD patterns.

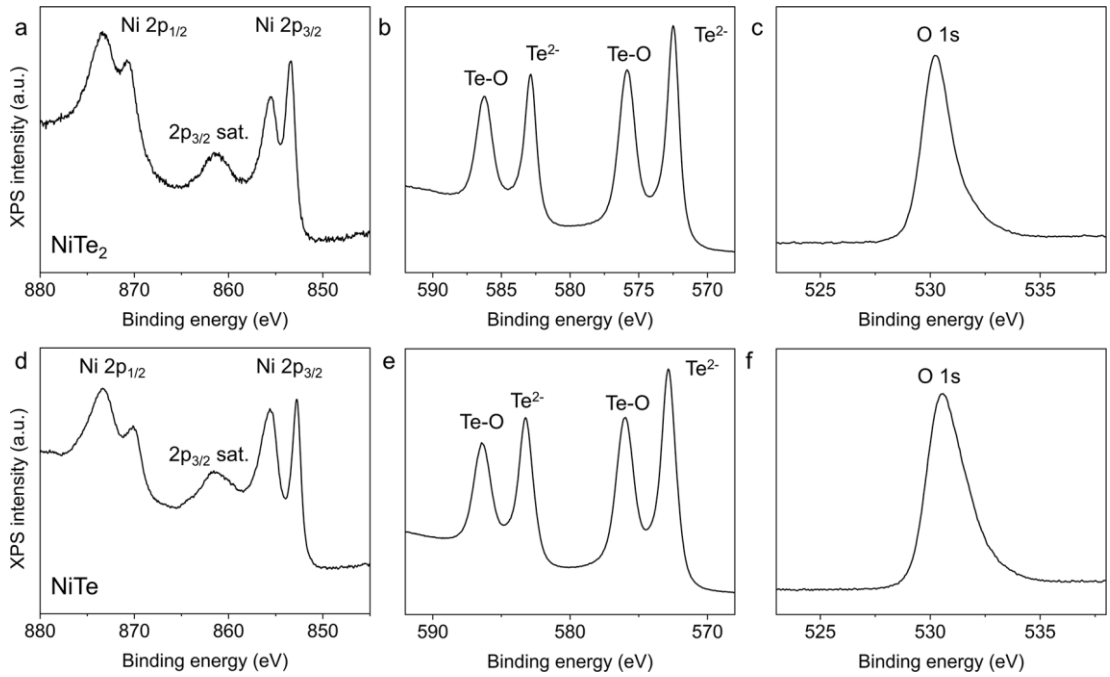

Fig. S6. XPS spectra of (a) Ni 2p, (b) Te 3d, (c) O 1s for $NiTe_2$ nanosheets. XPS spectra of (d) Ni 2p, (e) Te 3d, (f) O 1s for NiTe nanosheets.

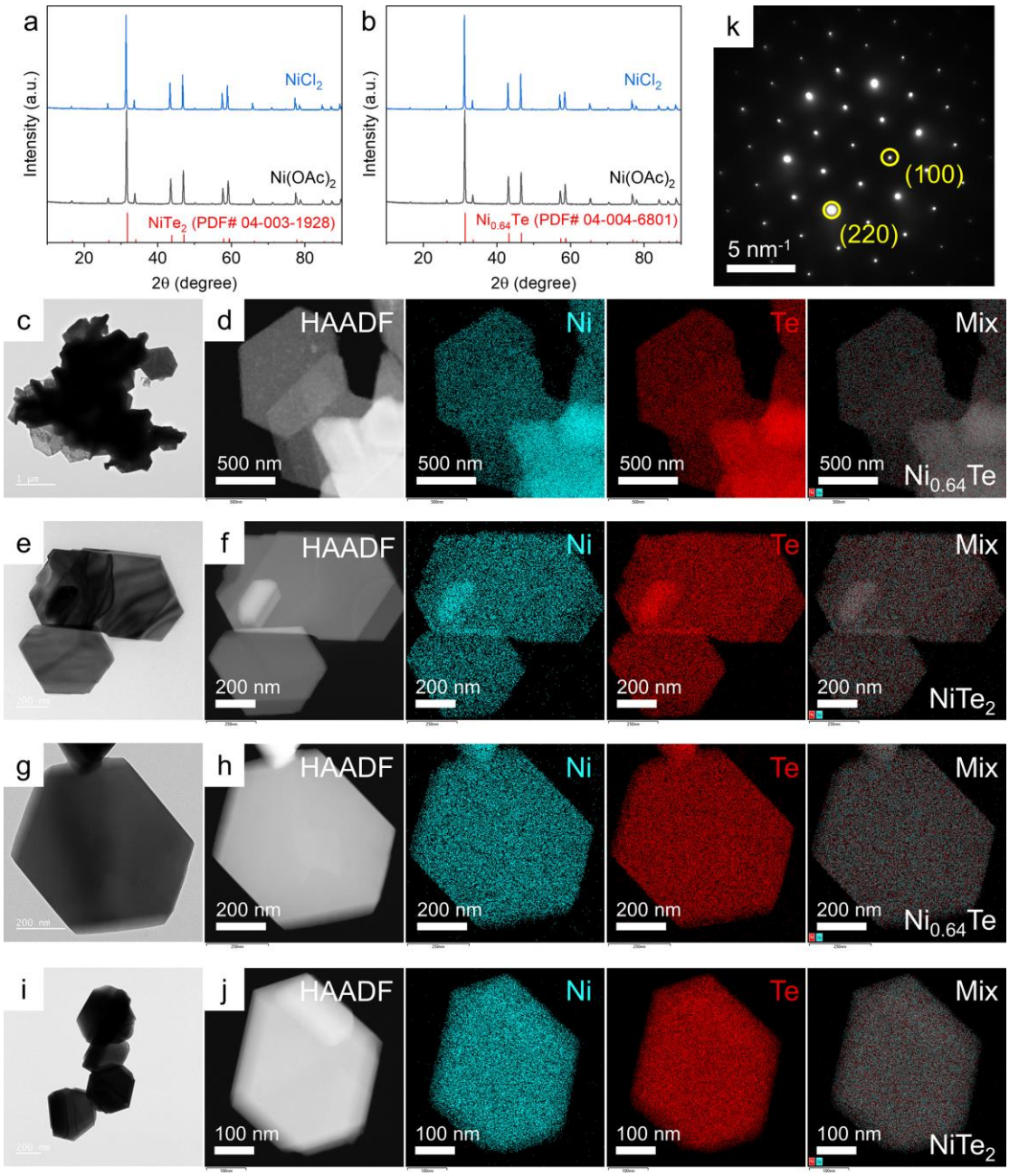

Fig. S7. XRD patterns of $NiTe_{2-x}$ nanosheets synthesized using $NiCl_2$ and $Ni(OAc)_2$ precursors: (a) $NiTe_2$ and (b) $Ni_{0.64}Te$. (c,d) TEM and HAADF images, and elemetal maps of Ni and Te of $Ni_{0.64}Te$ nanosheets synthesized using $NiCl_2$. (e,f) TEM and HAADF images, and elemetal maps of Ni and Te of $NiTe_2$ nanosheets synthesized using $NiCl_2$. (g,h) TEM and HAADF images, and elemetal maps of Ni and Te of $Ni_{0.64}Te$ nanosheets synthesized using $Ni(OAc)_2$. (i,j) TEM and HAADF images, and elemetal maps of Ni and Te of $NiTe_2$ nanosheets synthesized using $Ni(OAc)_2$. (k) Representative SAED pattern of $NiTe_2$ nanosheets synthesized using $NiCl_2$.

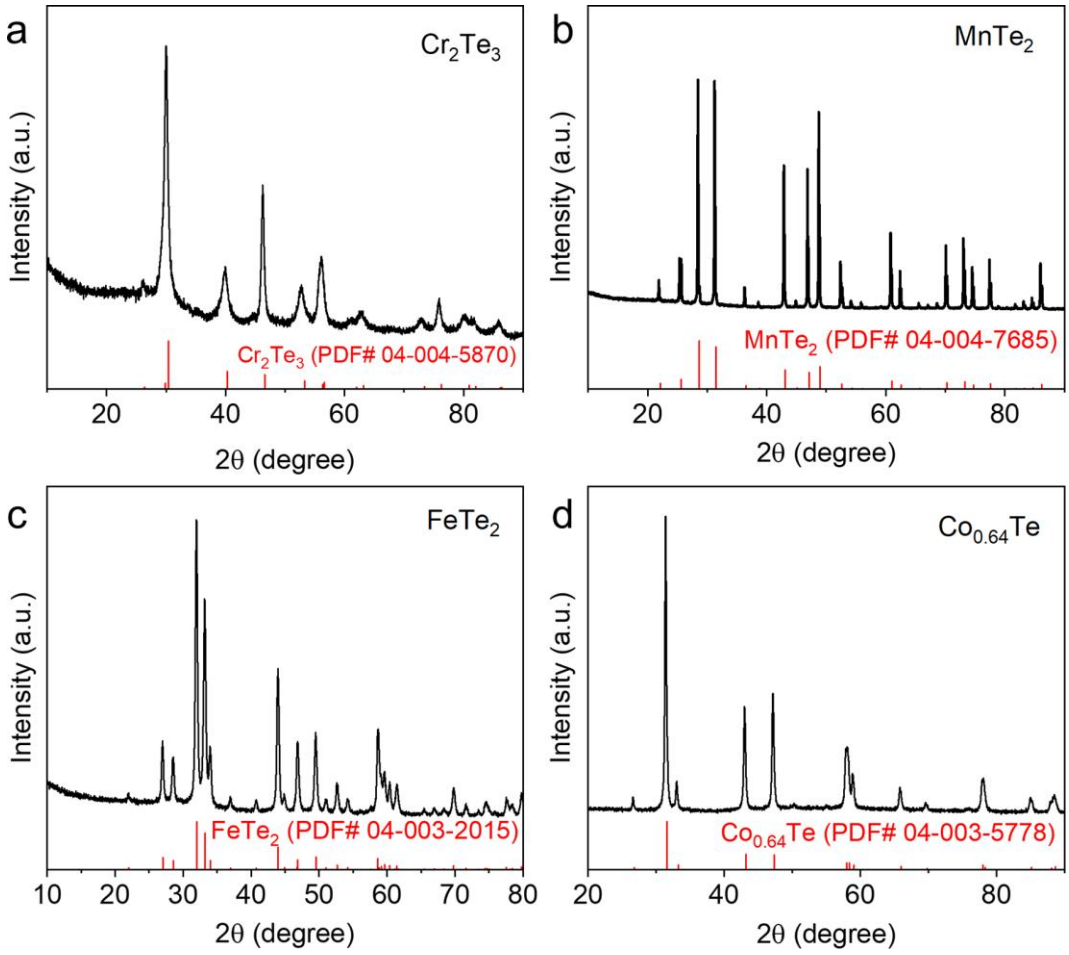

Fig. S8. XRD patterns of (a) Cr_2Te_3, (b) $MnTe_2$, (c) $FeTe_2$, and (d) $Co_{0.64}Te$.

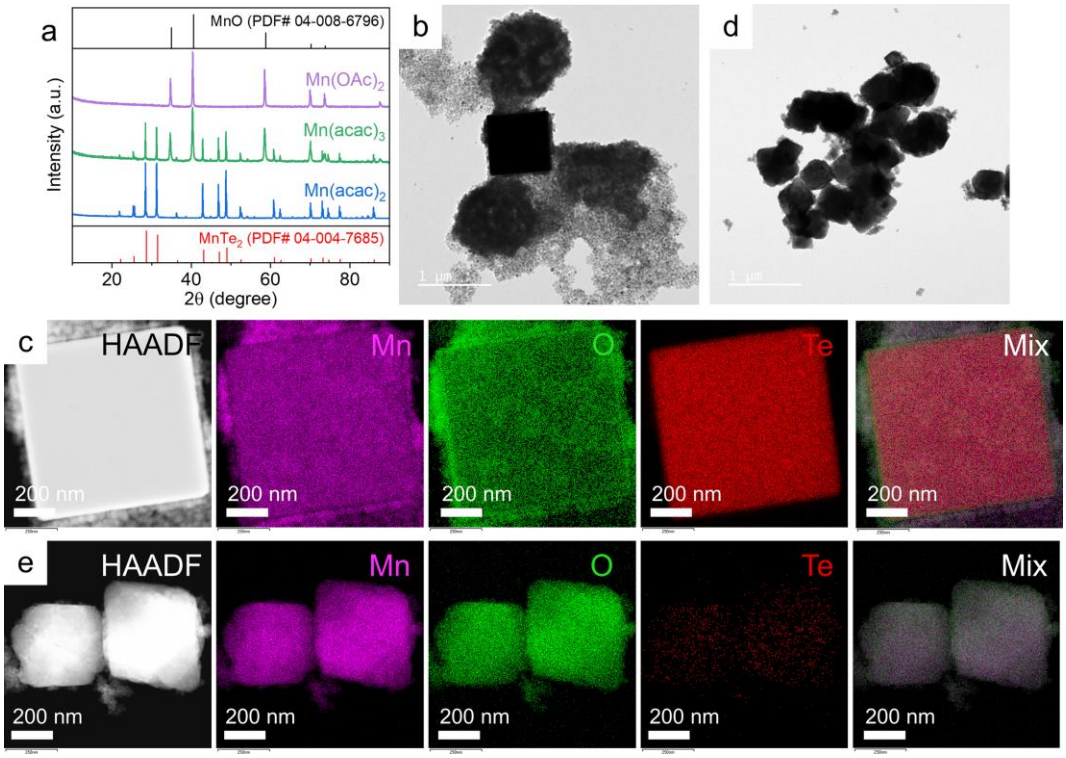

Fig. S9. (a) XRD patterns of the synthesis of the $MnTe_2$ nanocube using $Mn(OAc)_2$, $Mn(acac)_3$, and $Mn(acac)_2$ precursors: (b-c) TEM and HAADF images, and elemetal maps of Mn, O, and Te of the mixture of $MnTe_2$ nanocube and MnO nanoparticles synthesized using $Mn(acac)_3$. (d-e) TEM and HAADF images, and elemetal maps of Mn, O, and Te of the large MnO nanoparticles synthesized using $Mn(OAc)_2$.

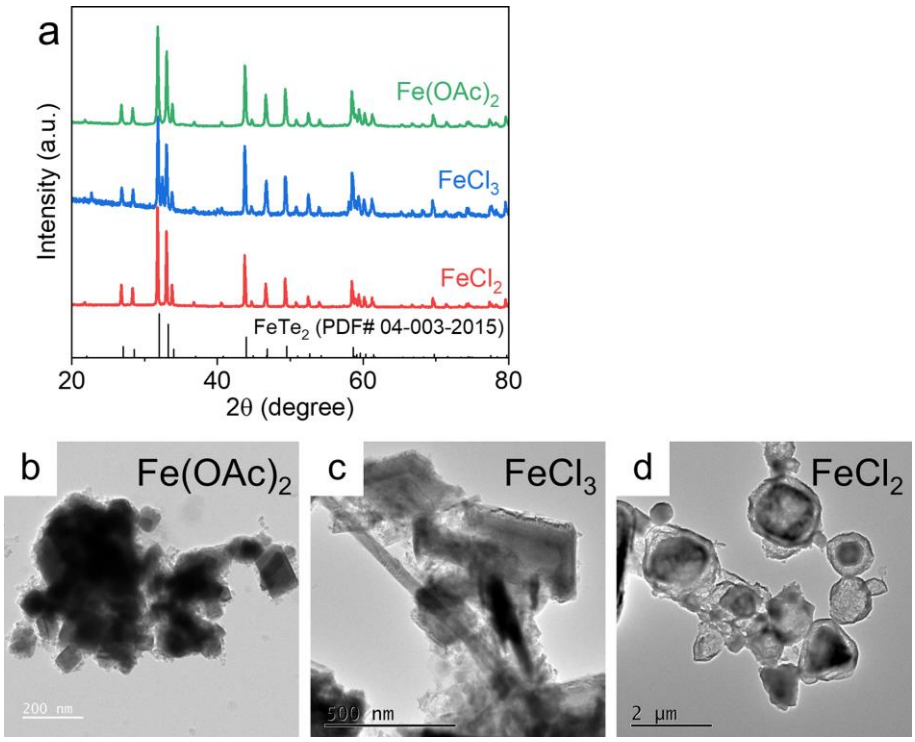

Fig. S10. (a) XRD patterns and TEM images of $FeTe_2$ NCs synthesized using (b) $Fe(OAc)_2$, (c) $FeCl_3$, and (d) $FeCl_2$ precursors, respectively.

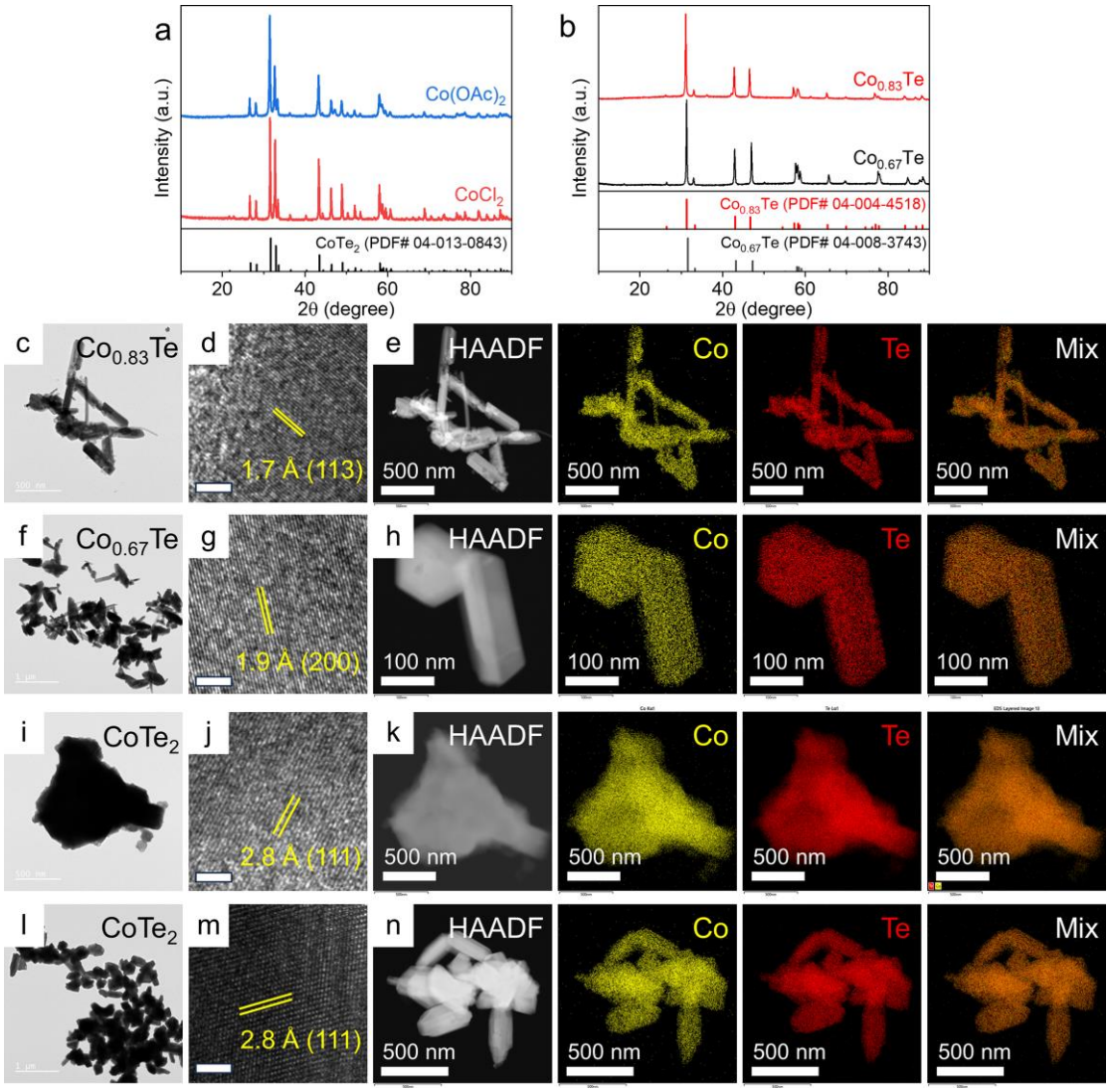

Fig. S11. XRD patterns of $CoTe_{2-x}$ nanoplates synthesized using $CoCl_2$ and $Co(OAc)_2$ precursors: (a) $CoTe_2$ and (b) $Co_{0.64}Te$ and $Co_{0.83}Te$. (c-e) TEM, HRTEM and HAADF images, and elemetal maps of Co and Te of $Co_{0.83}Te$ nanoplates synthesized using $Co(OAc)_2$. (f-h) TEM, HRTEM and HAADF images, and elemetal maps of Co and Te of $Co_{0.67}Te$ nanoplates synthesized using $Co(OAc)_2$. (i-k) TEM, HRTEM and HAADF images, and elemetal maps of Co and Te of $CoTe_2$ nanoplates synthesized using $CoCl_2$. (l-n) TEM, HRTEM and HAADF images, and elemetal maps of Co and Te of $CoTe_2$ nanoplates synthesized using $Co(OAc)_2$. Undefined scale bars: 2 nm.

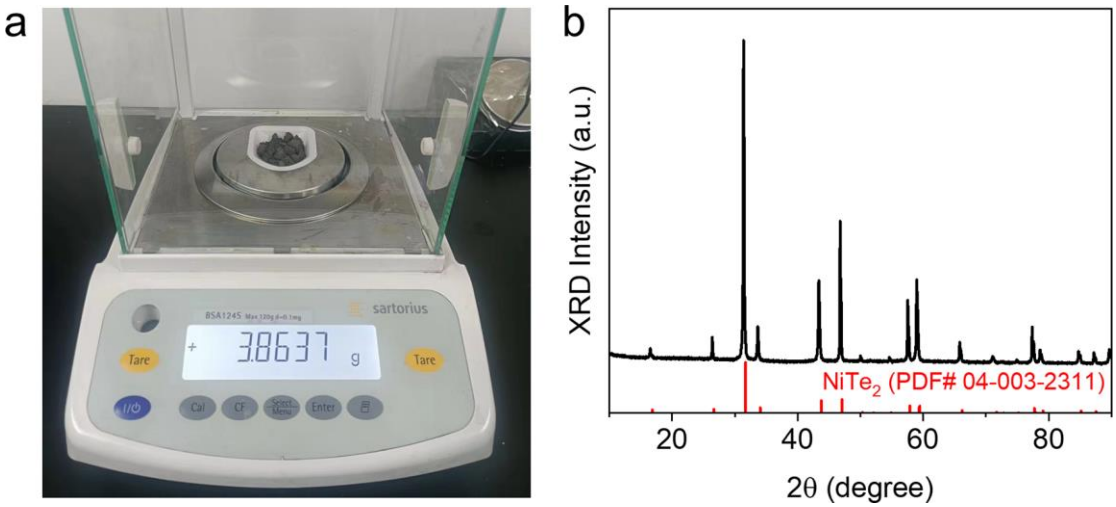

Fig. S12. (a) Photograph of $NiTe_2$ nanosheets powders produced by large-scale synthesis in a single batch. (b) XRD patttern of $NiTe_2$ nanosheets from scaled-up synthesis.

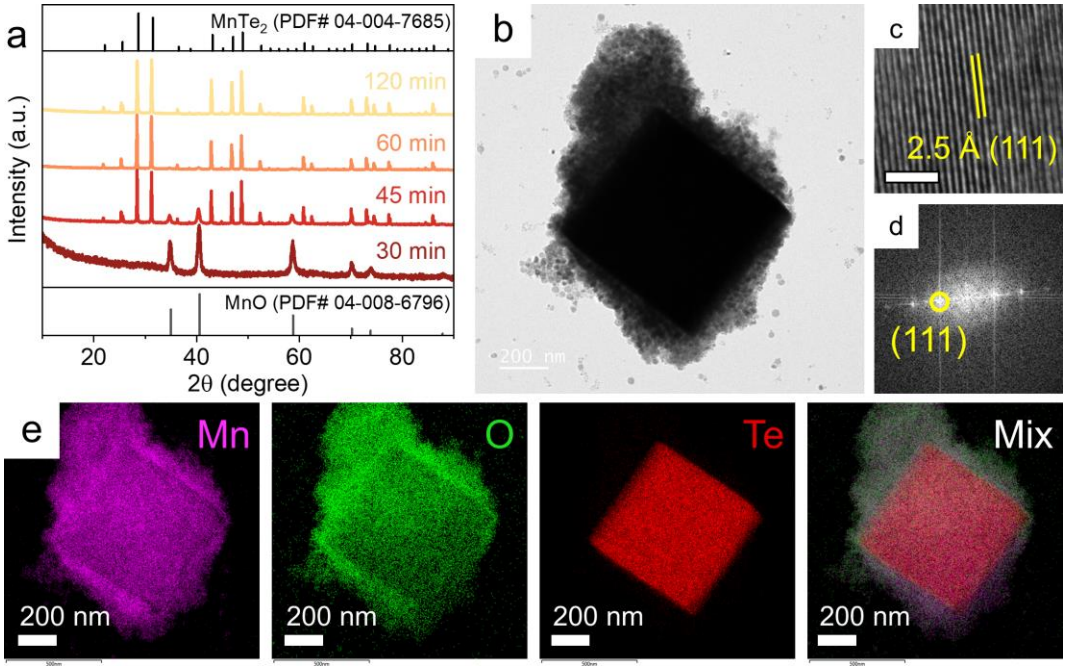

Fig. S13. XRD patterns of the transformation from MnO to $MnTe_2$ using Mn:Te ratio of 1:1.5. (b) TEM, HRTEM image, corresponding FFT pattern and elemental maps of Mn, O, and Te of MnO to $MnTe_2$ mixtures obtained at 45 min of the reaction. Undefined scale bars: 2 nm.

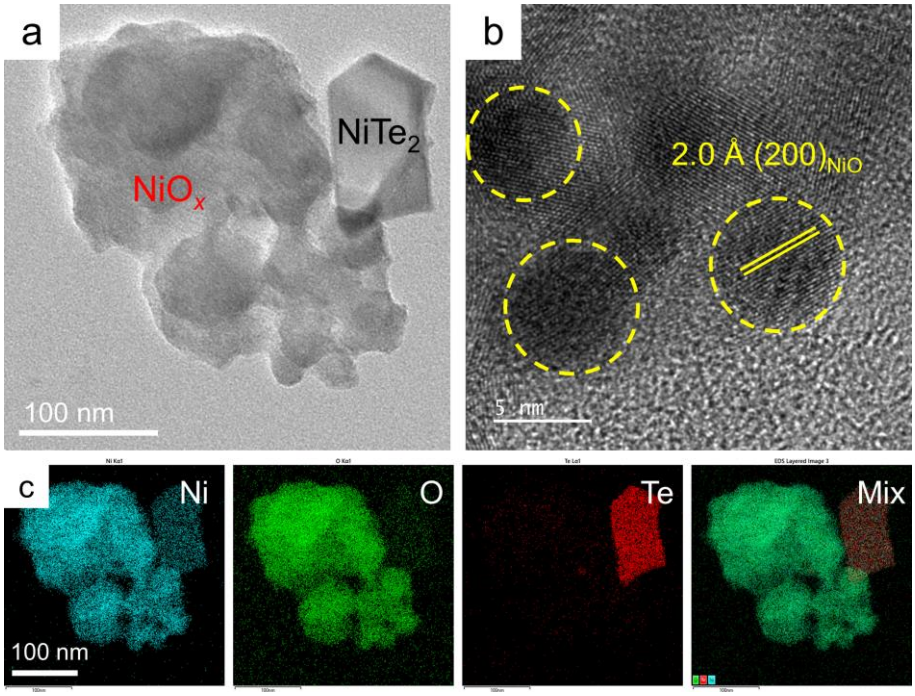

Fig. 14. (a) TEM image of the mixture of NiO_x and $NiTe_{2-x}$ NCs at the initial stage for the synthesis of $NiTe_2$, (b) HRTEM image of NiO_x intermediates, (c) elemental maps of Ni, O, and Te for the mixture of NiO_x and $NiTe_{2-x}$ NCs.

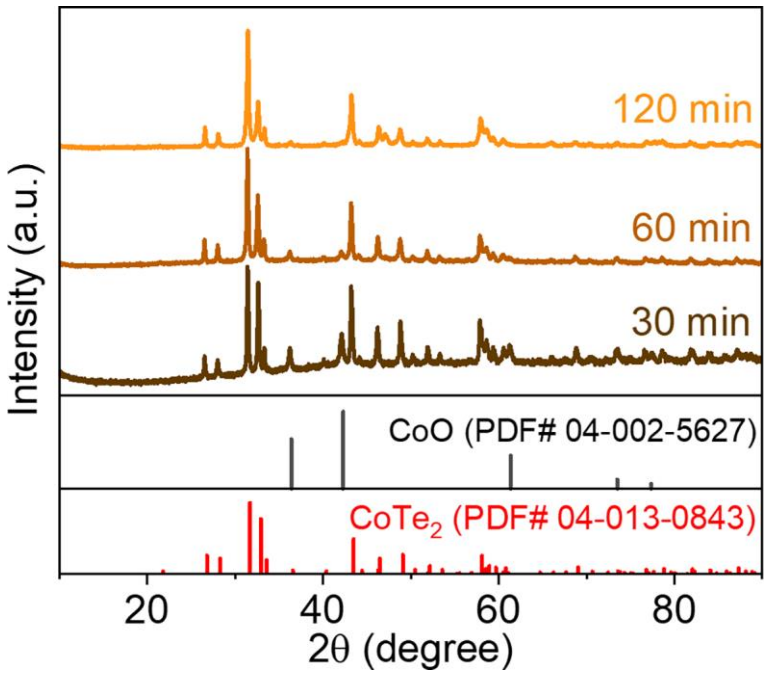

Fig. S15. XRD patterns aliquotes extracted from the synthesis of $CoTe_2$ nanoplates at different reaction times.

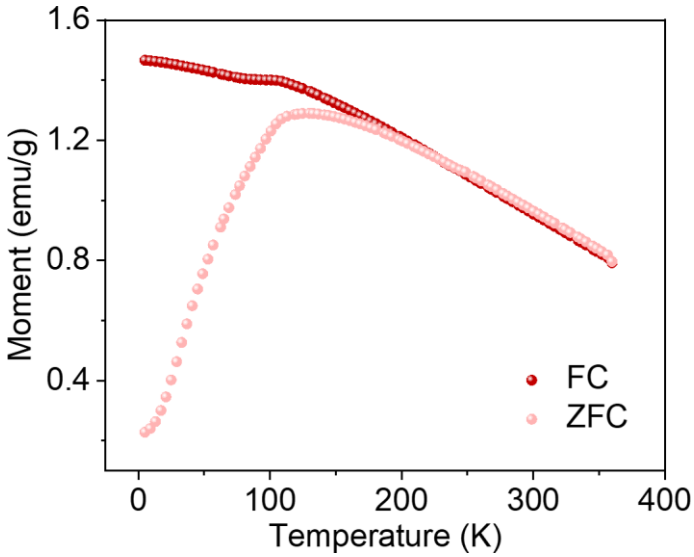

Fig. S16. M-T curve of $FeTe_2$.

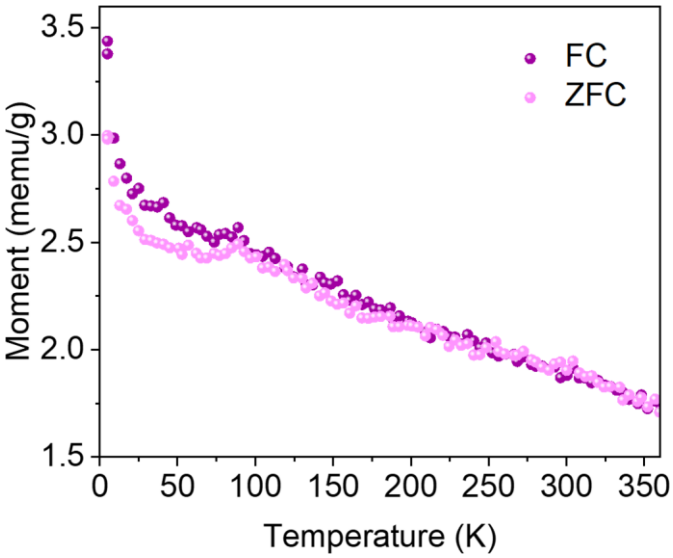

Fig. S17. M-T curve of $MnTe_2$.

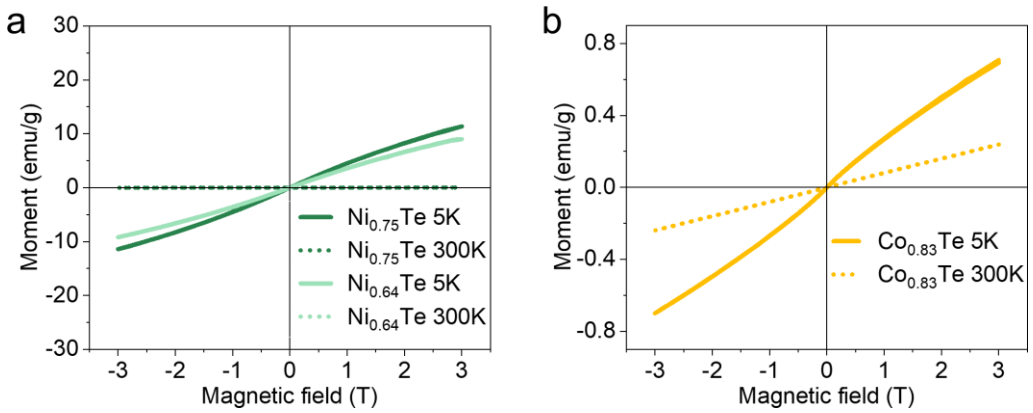

Fig. S18. M-T curve of (a) $Ni_{0.75}Te$ and $Ni_{0.64}Te$, (b) $Co_{0.83}Te$.